Analysis of the canonical turbulent shock front

Hui Cao[1], Tai Jin[2], Lipo Wang[1], Kun Luo[2] and Jianren Fan[2]
[1] UM-SJTU Joint Institute, Shanghai JiaoTong Univ.
Shanghai, China
[2] State Key Laboratory of Clean Energy Utilization, Zhejiang Univ.
Hangzhou, China

1 Introduction

The shock and turbulence interaction is of essential importance to understand the physics of supersonic turbulence. Physically, in the shock region the local fluid element is strongly compressed with a sharp change of the fluid parameters, e.g. temperature, pressure and density. In the turbulent supersonic flow, a key problem of interest is about the amplification factor, which focuses on the linkage between physical quantities in the upstream (supersonic) and downstream (subsonic) region. Based on a linearized analysis Anyiwo and Bushnell (1982) derived the amplification (or generation) function with respect to the turbulence disturbance. From such analysis they summarized different turbulence amplification mechanisms. Larsson, Lee and other collaborators performed a set of landmark direct numerical simulations (DNS) of the canonical shock/turbulence interaction in a series of works [2–4]. The important topics investigated include the relation of the dissipative scale in the upstream and downstream regions, the anisotropy evolution behind the shock front, different shock regimes, the jump relations across the shock front, e.g. the Reynolds stress, vorticity and enstrophy. The numerical results show that because of the shock action, the dissipative scale becomes much smaller downstream behind the shock front and the turbulent energy focuses more toward the small scale side.

Besides such trans-shock problems, a topic of fundamental importance is how the shock region will respond to any disturbance from the flow, either laminar or turbulent. Considering a corrugated surface, one of the most important geometrical parameters is the surface curvature (typically the mean curvature). Although the shock front distortion can be clearly observed and tentatively explained in terms of random focusing and defocusing of the front by the inhomogeneities in the medium [5], further quantitative results of the surface curvature need to be developed. The present work focuses on some primitive issues of the turbulent shock, including the shock identification, conditional statistics and the front curvature analysis.

2 Numerical simulations

The problem studied here is the canonical turbulent shock, i.e. interaction between a nominally planar shock with isotropic turbulence. The simulation of a steady shock wave [2] is performed in the Cartesian frame,

Correspondence to: lipo.wang@sjtu.edu.cn

where the velocity vector $\vec{v}$ is denoted in components as $[u, v, w]$ along (x, y, z) directions, respectively. The governing equations are solved in the nondimensionalized form. Specifically the coordinate $x^* = x/L_0$ (same for y and z), time $t^* = tu_0/L_0$, velocity vector $\vec{v}^* = \vec{v}/u_0$, density $\rho^* = \rho/\rho_0$, temperature $T^* = T/T_0$, dynamic viscosity $\mu^* = \mu/\mu_0$ and pressure $p^* = p/(\rho_0 u_0^2/\gamma)$, where L_0 is a reference scale, u_0 is the mean inlet velocity along x. To simplify the notation, the asterisk will be omitted hereafter. The dimensionless computation domain is set as $[-\pi, 2\pi] \times [0, 2\pi] \times [0, 2\pi]$, and the grid points are 1008, 384 and 384 along x, y and z, respectively. The mean flow is aligned with x. A planar shock wave at Mach number $M_0 = u_0/c_0 = 2$ is specified at $x = 0$, where the subscript 0 denotes the inlet value. A decaying isotropic turbulence pre-solved is then superimposed to the upstream uniform mean flow. Such a constructed field is swept as the inflow boundary condition using the Taylor's hypothesis. The standard nonreflecting boundary condition [6] is set at the outlet, and the periodic boundary condition is implemented along the lateral y and z directions. The stationary shock region is achieved by adjusting the specific back-pressure based on the Rankine-Hugoniot relation.

In the current work, an eighth-order-accurate version of a bandwidth-optimized WENO scheme (WENO-BO4) [7] is adopted to compute the convection terms, while the viscous terms are solved using the standard eighth-order central difference scheme. The temporal integration is calculated by the third order TVD Runge-Kutta multistage method. Physically the dissipative scale η across the shock region will largely decrease and then increase slowly along the downstream direction due to the turbulence decay. To efficiently resolve the turbulent structure, the equidistant grid is used in the two lateral directions, while a stretched mesh around the shock wave is adopted in the streamwise x direction. Let us and ds denote the immediate upstream and downstream of the shock wave, respectively. The relevant simulation parameters for both cases are listed in Tab. 1, including the inlet Reynolds number Re_λ based on the Taylor scale, the inlet laminar Mach number M_0 and inlet turbulent Mach number $M_{t,0}$, the upstream turbulent turbulent Mach number $M_{t,us}$, the upstream and downstream grid resolution in the vicinity of shock. For comparison, the inlet pressure remains the same for both cases.

Table 1: Characteristic parameters in DNS

grid	(x,y,z)	$Re_{\lambda,0}$	M_0	$M_{t,0}$	$M_{t,us}$	$\eta_{us}/\Delta x_{us}$	$\eta_{ds}/\Delta x_{ds}$
case 1	$1008 \times 384 \times 384$	37.8	2.0	0.13	0.114	2.14	1.16
case 2	$1008 \times 384 \times 384$	38.5	1.6	0.38	0.284	2.37	1.58

3 Shock identification and shock front curvature

Physically the shock region is thin with abrupt change of pressure, density and temperature. Near the shock the fluid element is strongly compressed and the velocity divergence assumes large negative values. Correspondingly the most widely used criterion of shock front identification is the local minimum velocity divergence [2, 3]. From the continuity equation the velocity divergence $-\nabla \cdot \vec{v} = D\rho/Dt/\rho$, where D/Dt represents the material derivative. Therefore the spatial points with large negative dilatation have the large variation of density ρ, and pressure as well, with respect to time. It is reasonable to identify the shock front as some representative pressure isosurface.

This idea is justified by the numerical results. Fig. 1 shows for case 2 for example the comparison of the shock fronts defined by the minimum dilatation method (a) and by the representative pressure isosurface (b). The arrows in the plots indicate the mean flow direction, i.e. from the upstream side with low pressure to

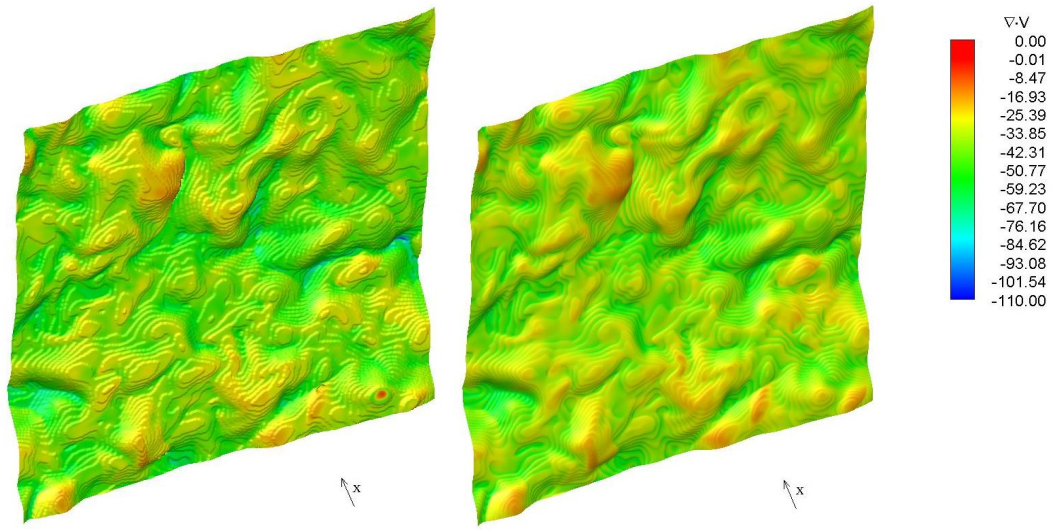

(a) (b)

Figure 1: The shock front identified by (a) the local minimal dilatation method; (b) the pressure isosurface (with $p = 1.45$), for case 2. The two fronts have highly identical structure and the distribution of the velocity divergence.

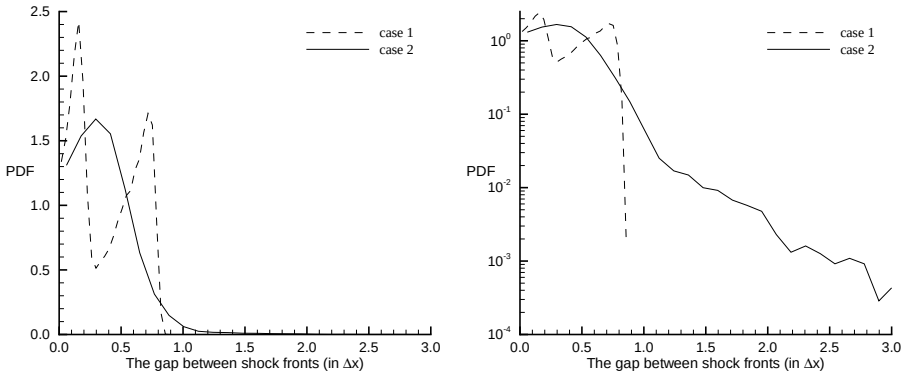

(a) (b)

Figure 2: PDF of the x coordinate difference between the shock fronts identified by two different methods (a) in the linear scale; (b) in the logarithmic scale.

the downstream side with high pressure. Both the geometrical structure and the distribution of dilatation are highly identical. When the shock front bends toward the high pressure (the downstream) side the local fluid is more compressed, whereas if the shock front bends toward the low pressure (upstream) side, the fluid is weakly compressed. Obviously the dilatation method generates the strong zigzag structure because the local minimum of $\nabla \cdot \vec{v}$ can appear only at grid points, i.e. such definition is resolution dependent. However, the iso-pressure method defines a much smoother shock front because of the pressure interpolation. Considering the experimental measurements, such iso-pressure definition is also meaningful because its easiness, compared with the velocity divergence measurement in an extremely thin shock region.

To further quantify the difference, Fig. 2 shows the PDF of the gap, i.e. the x coordinate difference, between the shock fronts defined by these two different methods, both in the linear and logarithmic scale. Clearly the probability of the gap beyond Δx is negligibly small; the location difference is almost confined within one grid cell δx, which is under the numerical resolution. Therefore it is convincing to claim the consistency between these two different shock identification criteria.

Because the fluctuating turbulent velocity, the shock front deviates from a planar surface as for the laminar case. Such surface distortion and the corresponding statistics are important to understand the turbulent shock. The most representative parameter to characterize surface geometry is the mean curvature κ, which can be expressed as $\kappa = -\nabla \cdot \vec{n}$, where n is the unit normal of the shock front. Based on the present shock identification, $\vec{n} = \nabla p/|\nabla p|$. For different pressure p its isosurface curvature assumes different statistics. For case 1 the PDF of κ conditional on different pressure isosurfaces is plotted in Fig. 3. Qualitatively the case 2 results are similar.

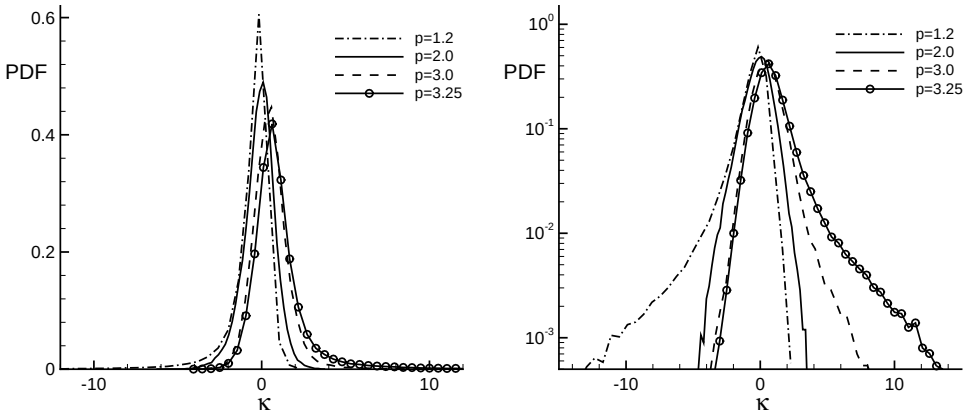

Figure 3: PDF of κ of the different pressure isosurfaces: (a) in the linear plot, (b) in the logarithmic plot.

With the increase of p the pressure isosurface shifts from upstream to downstream. At smaller p (e.g. $p = 1.2$) $PDF(\kappa)$ is negatively skewed, i.e. the isosurface bends towards the downstream side, whereas $PDF(\kappa)$ is positively skewed for larger p (e.g. $p = 3.0$), i.e. the isosurface bends towards the upstream side. At some intermediate value (e.g. $p = 2.0$) the PDF is almost symmetric.

Such asymmetry tendency can clearly be presented in Fig. 4, where the pressure isosurface is color mapped with the curvature value, viewing from the downstream side. When pressure increases, with the same color scale the positive curvature part becomes more dominant, whereas the negative curvature part shrinks. This visualization agrees with the PDF results in Fig. 3.

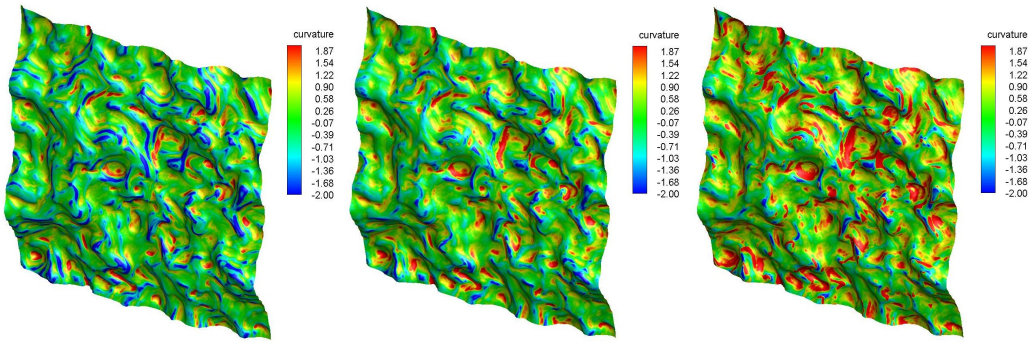

(a) (b) (c)

Figure 4: The spatial distribution of curvature on different pressure isosurfaces at the same color scale for case 1 with (a) $p = 2.0$ (b) $p = 2.5$ (c) $p = 3.0$. For the purpose of clear visualization the x coordinate (shock normal) has been stretched.

4 Kinematic influence of turbulence on the shock front

Kinematically the upstream fluctuating velocity leads to the corrugation of the shock front. It is important to understand such relation in between. We introduce the shock speed u_s, which is defined as

$$u_s = (\vec{v}_u - \vec{v}_p) \cdot \vec{n}, \tag{1}$$

where $\vec{v}_u$ is the local fluid velocity on the upstream side, $\vec{n}$ is the unit normal of the pressure isosurface, $\vec{v}_p$ is the Lagrangian velocity of the iso-pressure surface satisfying $\dfrac{\partial p}{\partial t} + \vec{v}_p \cdot \nabla p = 0$. The physical meaning of u_s is the relative velocity along the shock normal direction between the shock front velocity and the fluid velocity on the upstream side.

The distortion of the shock front is a cumulative effect of the turbulent shock speed. Typically the shock excursion is relatively small, i.e. the local shock normal $\vec{n} \sim [1, 0, 0]$ and thus the local fluid velocity $\vec{v}_u$ can be represented by its component u along x. Fig. 5 shows the relation between u_s and u. There exists a strong positive correlation, i.e. the larger u leads to the larger shock speed u_s. The conditional mean of u_s, denoted as $\langle u_s \rangle$, is almost linearly dependent on u. The solid dot in the figure indicates the reference state of the laminar shock case, which has only one u and u_s. The slope of the $\langle u_s \rangle$ curve is smaller than one, which means that physically there is some negative feedback of the shock dynamics on the disturbance from turbulence, i.e. the retarded response of the shock front motion to the local fluid motion, whose detailed mechanism need to be further investigated. In addition, the variation of u_s at different u is almost constant, which means for different velocity u the fluctuation of u_s is almost invariant.

5 Concluding remarks

The shock front has been newly defined in the present work by the representative pressure isosurface, showing good agreement with the existing minimum dilatation criterion. Topologically the turbulent shock front deviates from being planar because of the disturbance from the flow field, which is the kinematic effect from the turbulent shock speed quantity. Numerical results show that this speed varies almost linearly with the

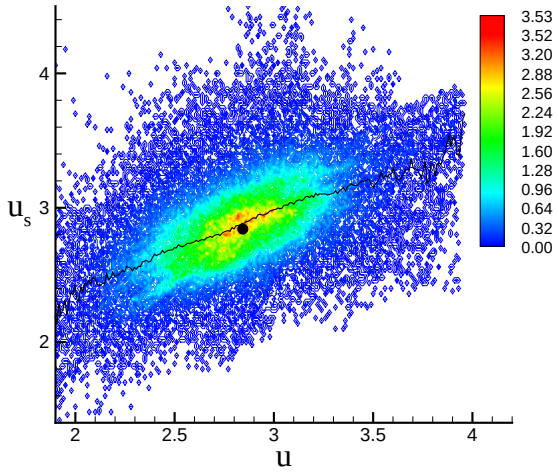

Figure 5: Dependence of the shock speed u_s on the flow velocity u on the upstream side. The solid dot is the reference state for the laminar case.

local fluid velocity. The fact that the linearity coefficient is small than unity can be explained physically by the retarded response of the shock motion to the fluid fluctuation.

References

[1] Anyiwo J. C., Bushnell D. M., Turbulence amplification in shock-wave boundary-layer interaction[J]. AIAA Journal 1982, 20(7): 893-899.

[2] Larsson J, Lele S. K., Direct numerical simulation of canonical shock/turbulence interaction[J]. Phys. Fluids 2009: 21(12) 126101.

[3] Lee S., Lele S. K., Moin P., Direct numerical simulation of isotropic turbulence interacting with a weak shock wave[J]. J. Fluid Mech. 1993, 251: 533-562.

[4] Larsson J., Bermejo-Moreno I., Lele S. K., Reynolds- and Mach-number effects in canonical shock-turbulence interaction[J]. J. Fluid Mech. 2013, 717: 293-321.

[5] Hesselink L., Sturtevant B., Propagation of weak shocks through a random medium[J]. J. Fluid Mech. 1988, 196: 513-553.

[6] Yoo C. S., Im H. G., Characteristic boundary conditions for simulations of compressible reacting flows with multi-dimensional, viscous and reaction effects[J]. Combust. Theor Model. 2007, 11(2): 259-286.

[7] Martin M. P., Taylor E. M., Wu M., Weirs V. G., A bandwidth-optimized WENO scheme for the effective direct numerical simulation of compressible turbulence[J]. J. Comput. Phys. 2006, 220(1): 270-289.